Case Studies in Thermal Engineering 32 (2022) 101907

Contents lists available at ScienceDirect

Case Studies in Thermal Engineering

journal homepage: www.elsevier.com/locate/csite

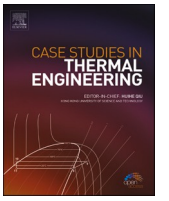

Modelling fire smoke dynamics in a stairwell of high-rise building: Effect of ambient pressure

Junjiang He [a,c], Xinyan Huang [b,**], Xiaoyao Ning [a], Tiannian Zhou [a], Jian Wang [a,*], Richard Kwok Kit Yuen [c]

[a] State Key Laboratory of Fire Science, University of Science and Technology of China, Hefei, China
[b] Department of Building Environment and Energy Engineering, Hong Kong Polytechnic University, Hong Kong, China
[c] Department of Architecture and Civil Engineering, City University of Hong Kong, Hong Kong, China

ARTICLE INFO

Keywords:
Smoke dynamics
Pressure effect
High-rise building
Full-scale stairwell

ABSTRACT

In a high-rise building fire, vertical shafts are the main paths for hot smoke to spread to multiple floors, posing a significant fire hazard. In this work, the large eddy simulation (LES) was applied to simulate smoke dynamics in a full-scale stairwell and study the influence of ambient pressure and heat release rate (HRR). The results have shown that the air mass flow rate into the stairwell decreases as ambient pressure drops on account of the lower air velocity and density and increases with HRR because of the stronger stack effect and increased smoke production. An equation incorporating ambient pressure and HRR is proposed for predicting the air mass flow rate. The temperature of hot smoke near the fire source increases with the reduced ambient pressure, while on the floors away from the fire source, the temperature decreases due to the higher temperature attenuation at a lower pressure. In addition, an empirical model is put forward for predicting the rising time of the smoke plume considering ambient pressure. The results could increase the basic understanding of smoke movement mechanisms and contribute to engineering applications of smoke control in high-rise building fires under reduced ambient pressure conditions.

1. Introduction

In the last few decades, numerous high-rise buildings have been erected worldwide with the rapid growth of population and the continuous shortage of land sources. Meanwhile, the increased fire safety problems associated with high-rise buildings have aroused a broad public concern. A notable event is the Garley building fire which happened in Hong Kong in 1996, resulting in 41 fire fatalities and 80 injuries [1]. Toxic smoke is the greatest threat to people's evacuation than the fire itself [2,3], and attributes to roughly 85% of the fatalities in the fire from the statistical analysis [4,5]. There are many vertical shafts, including elevator wells, stairwells, ventilation ducts and cable shafts, which connects multiple floors of high-rise buildings. During high-rise building fires, the above vertical channels may become the main paths for toxic smoke to spread to non-fire floors [6–8]. The vertical movement of hot smoke in vertical shafts is mainly driven by two mechanisms, the turbulent mixing and stack effect [9–12]. The stack effect (or chimney effect) is formed as a result of the density differences between the air outside of the shafts and the gas inside the shafts [13,14], while the turbulent mixing is in relation to the Rayleigh-Taylor instability [15,16].

* Corresponding author.
** Corresponding author.
E-mail addresses: xy.huang@polyu.edu.hk (X. Huang), wangj@ustc.edu.cn (J. Wang).

https://doi.org/10.1016/j.csite.2022.101907
Received 12 September 2021; Received in revised form 22 November 2021; Accepted 2 March 2022
Available online 4 March 2022

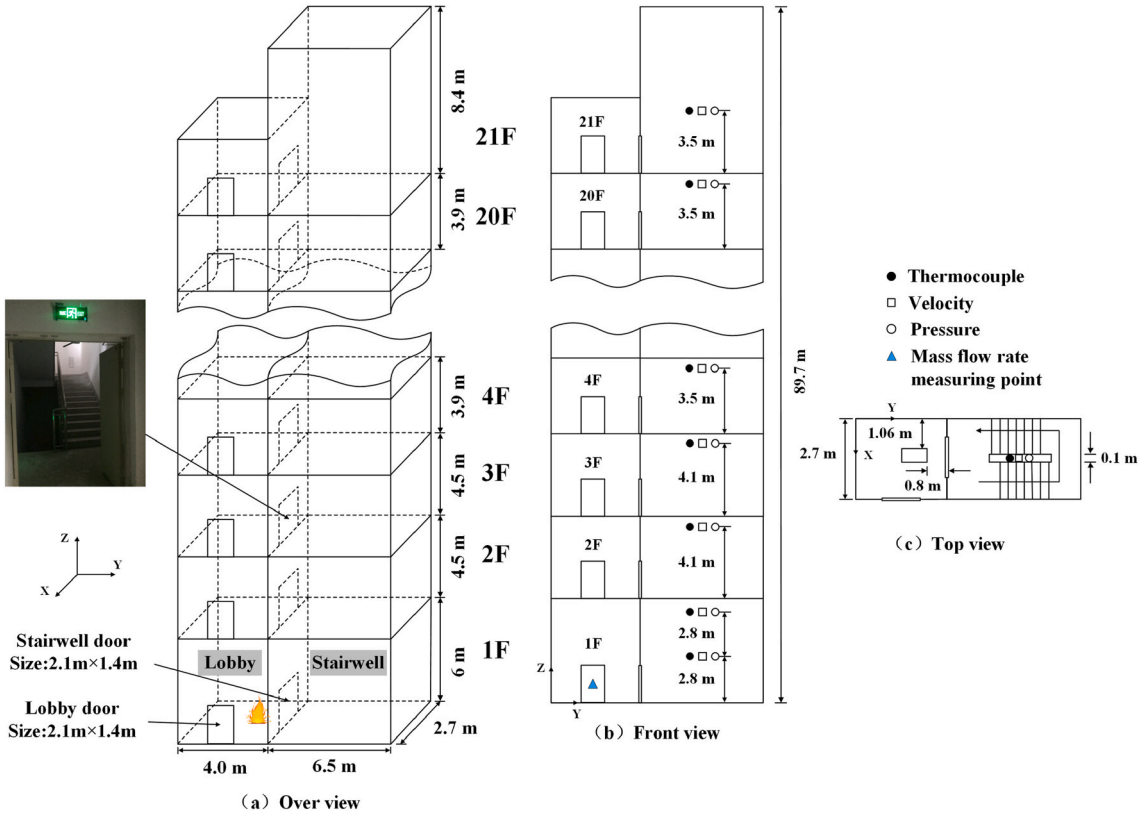

Fig. 1. The schematic of 21-story full-scale building model.

Many researchers around the world have investigated the smoke dynamics under the stack effect in high-rise building fires. For example, Marshall [17,18] investigated smoke dynamics in scale models of the five-story stairwell and shaft and established computer programs to quantify the air entrainment. Zhang et al. [7] numerically studied the neutral pressure plane position under the stack effect in a shaft and put forward a new theoretical model to predict it. Su et al. [10] investigated the smoke dynamics in a five-story building, and the results found that the open of top door at the attic stairwell would enhance the stack effect and hasten the visibility decrease and temperature increase in the stairwell. Chen et al. [11] numerically investigated smoke dynamics and neutral pressure plane position in a vertical shaft under different locations of heat sources. The results showed that the location of heat sources had a great significance on smoke movement and neutral plane position and a series of empirical models for predicting neutral plane positions considering multi-heat sources were proposed. Li et al. [12] conducted full-scale numerical simulations to study the smoke dynamics in a semi-open vertical shaft and showed that the thermal plumes were moved away from the center of the shaft by the supplement airflow because one side of the shaft was open. Black [13] used COSMO program to study the smoke dynamics during building fires and found that the outside temperature had a relatively small effect on the neutral pressure plane, and the top vent area of the shaft greatly influenced the smoke movement in the building. Shi et al. [14,19] introduced a 1/3 scale 12-storey stairwell to study the impact of ventilation state on the temperature distribution and airflow velocity. Gao et al. [20] studied airflow and flame shapes of fire source under the stack effect and put forward the relationship between the dimensionless airflow velocity, opened window height and heat release rate of the fire source. Zhu et al. [21] studied the smoke dynamics and temperature distribution under different velocities of external wind in a shaft and found external side wind could enhance the fire burning and smoke spreading. Ahn et al. [3] numerically and experimentally investigated the transport phenomena of hot smoke inside high-rise stairwells under various open window scenarios and found that the smoke movement was slowed by the intake air through open windows. He et al. [22] experimentally investigated the influence of upper opening location on the smoke dynamics and temperature stratification in a full-scale stairwell and the results showed that the stairwell was separated into two regions by the upper opening where the movement mechanisms and temperature distribution of hot smoke were different. In the lower region, both the stack effect and turbulent mixing dominated in the movement of hot smoke, whereas in contrast, in the upper region, turbulent mixing play an important role.

However, all those previous studies on smoke dynamics in high-rise building fires were carried out at about 1 atm near sea level. In the past few years, the number of high-rise buildings at high altitude areas has increased, such as the Colorful Auspicious Tower (303 m) in Qinghai, China, where the ambient pressure is about 77 kPa. As the ambient pressure decreases with the increasing altitude, the air density is smaller at higher altitude areas, which directly affects smoke dynamics and stack effect in high-rise buildings. So far, the influence of reduced pressures on smoke characteristics in full-scale high-rise buildings has not been investigated.

This study is aimed to study the impact of the ambient pressure on fire smoke dynamics and vertical temperature, velocity and hot

Table 1
The numerical simulation details.

No.	HRR (MW)	P (kPa)
1–6	0.5	50, 60, 70, 80, 90, 101
7–12	1.0	50, 60, 70, 80, 90, 101
12–18	1.5	50, 60, 70, 80, 90, 101
19	0.36	101
20	0.84	101

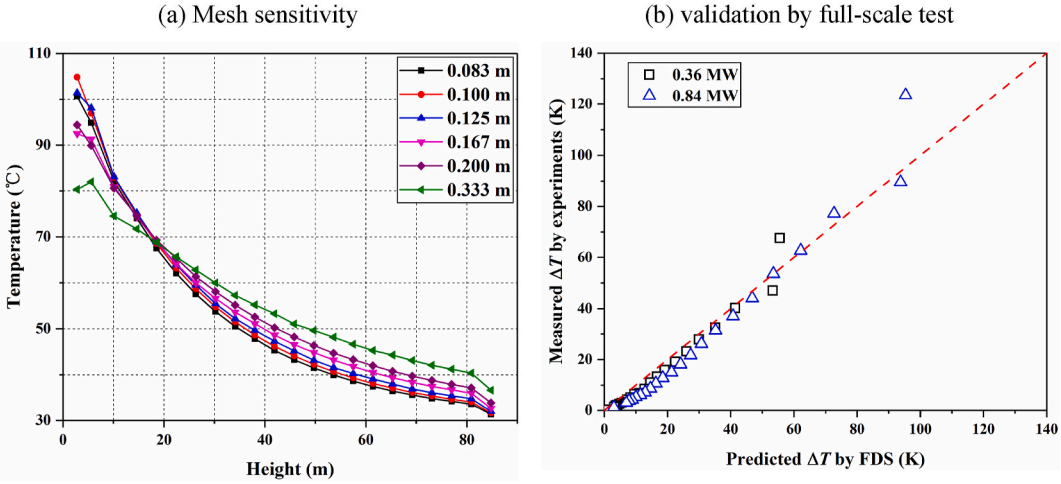

Fig. 2. (a) The temperature distributions at the vertical centerline of the stairwell under different grid sizes, and (b) comparison between the numerical results and the previous full-scale test results [22].

pressure distributions induced by the stack effect in a stairwell of high-rise buildings. A numerical method was employed to build a full-scale model, and the proposed model is validated by the previous real-scale fire experiments [22].

2. Numerical model

2.1. Physical model

The typical 21-story high-rise commercial building in Ref. [22] was used as a reference to build a full-scale numerical model. Fig. 1 illustrates the schematic of the numerical building model, consisting of the stairwell and lobby. The total height of the stairwell is 89.7 m, of which the heights of 1 F (ground), 2 F, 3 F, and 21 F are 6 m, 4.5 m, 4.5 m, and 8.4 m, respectively, and the heights of the remaining floors are all 3.9 m. The cross-section of the lobby and stairwell and are 4 m × 2.7 m and 6.5 m × 2.7 m, respectively. The size of the doors which connect the stairwell, lobby, and surroundings is 2.1 m high and 1.4 m wide. The construction material of the building is made of "Concrete", whose properties are as follows: the conductivity is 1.2 W/(m K), the specific heat is 0.88 kJ/(kg K), and the density is 2,200 kg/m^3 [23].

A column of 22 thermocouples, velocity and pressure sensors was located at the centerline of the stairwell to measure the temperature, velocity and pressure distributions of hot smoke. The device measuring the air mass flow rate entering the lobby was located centrally at the open lobby door of the ground floor. The lobby and stairwell doors on the 1 F and 21 F were always kept open in the model, while other doors were kept closed. The fire source that uses the ethanol as fuel was located 80 cm away from the stairwell door in the lobby of the ground floor, which is the same as the previous full-scale experiments. This fire source was basically modelled as a surface burner with varying fuel mass rates and a constant area of 0.5 m^2. Three fire heat release rates (HRRs) of 0.5 MW, 1.0 MW and 1.5 MW were set. The ambient pressure was varied as 50 kPa, 60 kPa, 70 kPa, 80 kPa, 90 kPa, and 101 kPa. In total, 20 cases were modelled. The numerical settings are presented in Table 1. Another two validation cases with the HRR of 0.36 MW and 0.84 MW at normal pressure were modelled first to ensure the model agreeing with the experimental data in Ref. [22]. In all cases, the ambient temperature was set to 30 °C.

2.2. CFD numerical solver

The numerical tool, Fire Dynamics Simulator (FDS) version 6.7.5 developed by NIST [24], was applied in this work to establish a physical model and solve governing equations. The LES turbulent solver is selected for this study which has been validated in the previous literature [3,25–29]. Past studies have demonstrated that FDS can give a good prediction of the smoke movement, O_2, CO_2 and CO concentrations, and temperature and velocity profiles in shafts and stairwells [25–27]. Ahn et al. [3] simulated the smoke dynamics in 12-storey building, where the modelled smoke flow temperature and velocity agreed well with experimental data.

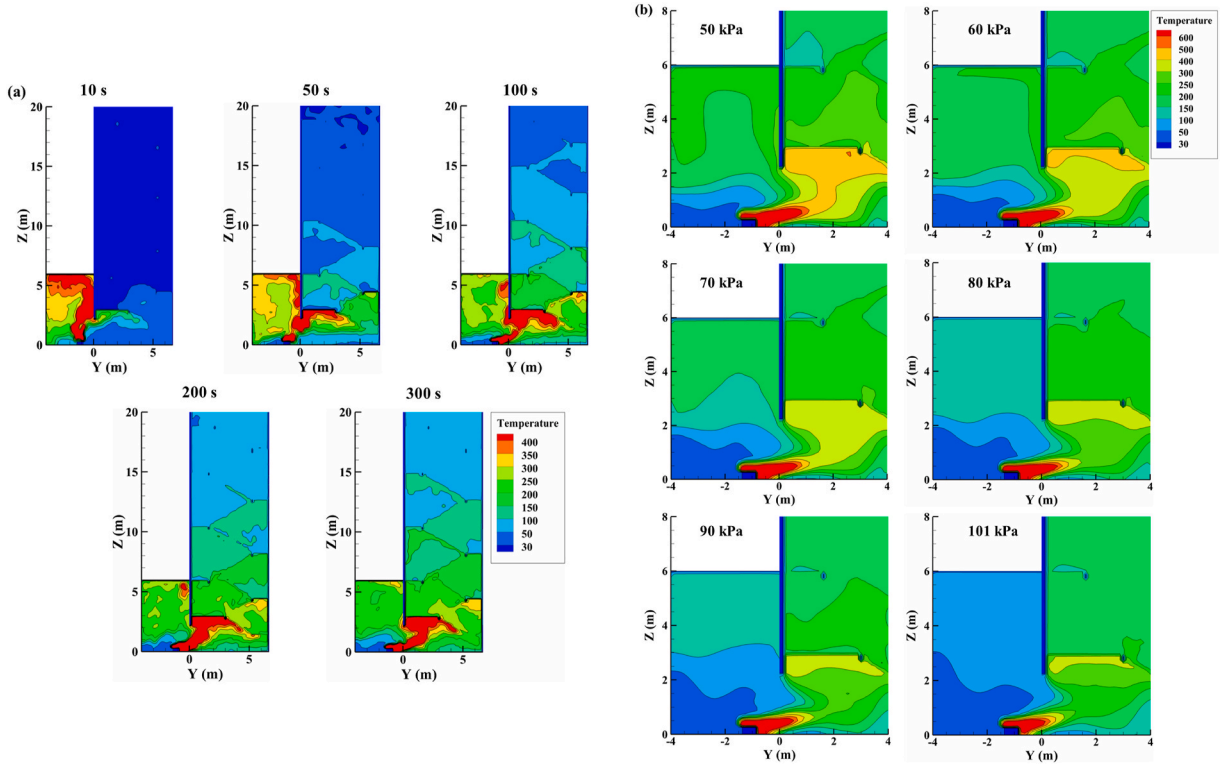

Fig. 3. (a) The evolution of temperature profiles at x = 1.35 m in the stairwell over time at 50 kPa, and (b) flame shapes on the fire floor under different ambient pressures for HRR of 1.5 MW.

2.3. Mesh size sensitivity analysis

From the FDS user guide [24], the ration $D^*/\delta x$ is employed as a criterion to assess the mesh sensitivity, where δx is the mesh size and D^* is the fire characteristic diameter which can be expressed by

$$D^* = \left(\frac{\dot{Q}}{\rho_a C_p T_a \sqrt{g}}\right)^{\frac{2}{5}} \tag{1}$$

It is suggested by the guide that the ration $D^*/\delta x$ is supposed to range from 4 to 16. For example, the case of HRR = 0.5 MW at 101 kPa gives $D^* = 0.73$ m, so that the mesh size is within the range of 0.05 m–0.18 m.

In general, the smaller the mesh size, the more accurate the numerical results will be, but more computation resources will be wasted, resulting in a lot of waste of time, and even leading to non-convergence of the calculation. In this pilot study, six different mesh sizes (0.083 m, 0.100 m, 0.125 m, 0.167 m, 0.200 m, 0.333 m) are compared. Meanwhile, the computational domains near the bottom and top openings are extended by 1 m to ensure accurate numerical data, which is suggested by the previous study [30]. Fig. 2(a) shows the grid sensitivity of modelled smoke temperature distribution along the stairwell, where simulation results between the mesh sizes of 0.083 m, 0.100 m and 0.125 m are closed. Therefore, 0.125 m is chosen as the mesh size in numerical simulations to balance the computational accuracy and time.

To validate the agreement of simulation results, the temperature ΔT at the centerline of the stairwell in Ref. [22] is applied to make comparisons between the full-scale tests and current simulations. The selected experiments involving different HRRs, 0.36 MW and 0.84 MW, with doors on 1 F and 21 F are open, which were repeated twice in a relatively stable environment. Fig. 2(b) shows the comparison between the numerical results and full-scale test results. It is obvious that the modelled temperatures are in good agreement with the experimental data, which supports the chosen grid resolution is fine enough, and the model is a good representative of full-scale fire tests.

3. Results and discussion

3.1. Flame shape and air flow

Fig. 3(a) plots the evolution of temperature profiles at x = 1.35 m in the stairwell, varying with time for ambient pressure of 50 kPa and HRR of 1.5 MW. It can be found that at the beginning, the flame burns straight and steadily. The hot smoke produced by pool fire flows upward under the buoyancy and impinges the ceiling of the lobby. After the hot smoke fills the lobby, it begins to flow into the stairwell and rises up in a spiral, driven by the stack effect. As the burning continues, increasing amount of smoke spreads into the

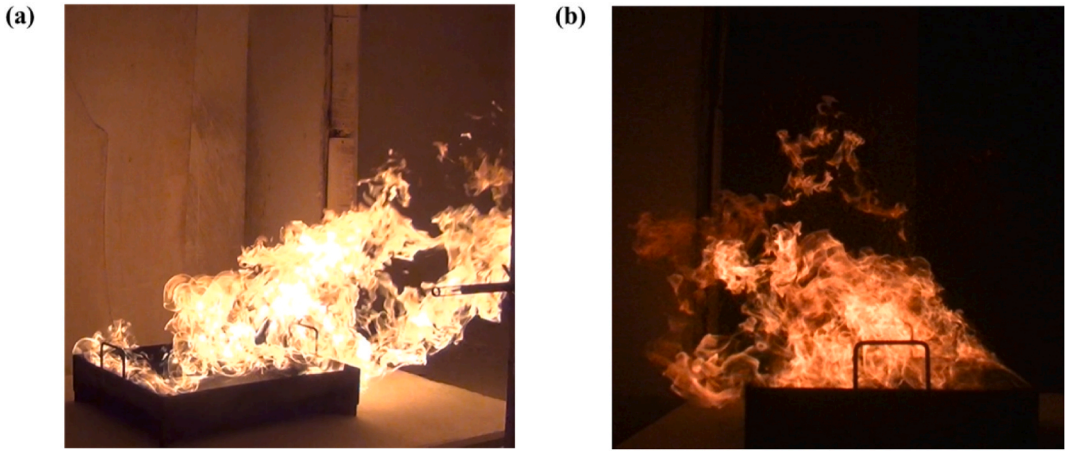

Fig. 4. The flame shapes from previous full-scale study [22], (a) front view and (b) side view.

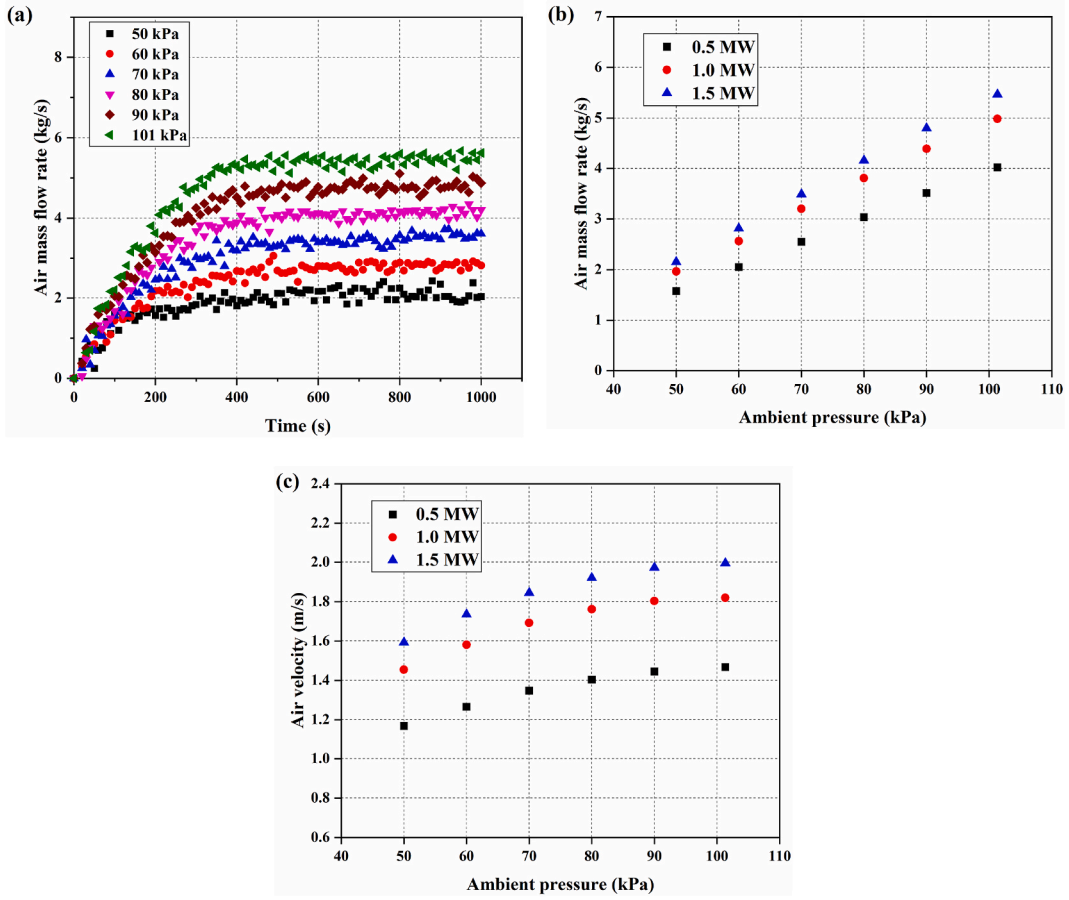

Fig. 5. (a) Air mass flow rates through the lobby door over time for HRR of 1.5 MW, (b) average air mass flow rate, and (c) calculated air velocity during the steady-state stage for all cases.

stairwell, which intensifies the stack effect. Then the flame starts to incline towards the direction of the stairwell door as a result of the supplement air flowing into the lobby. Moreover, as shown in Fig. 3(a), the temperature of hot smoke at the ceiling of the lobby keeps dropping over time, and the high-temperature zone gradually transfers from the lobby into the stairwell due to the stack effect.

Rew and Deaves [31] suggested that the characteristic temperature of the flame boundary is 600 °C through full-scale fire experiments. Based on it, the high-temperature continuous flame shape can be obtained from the temperature profiles on the fire floor.

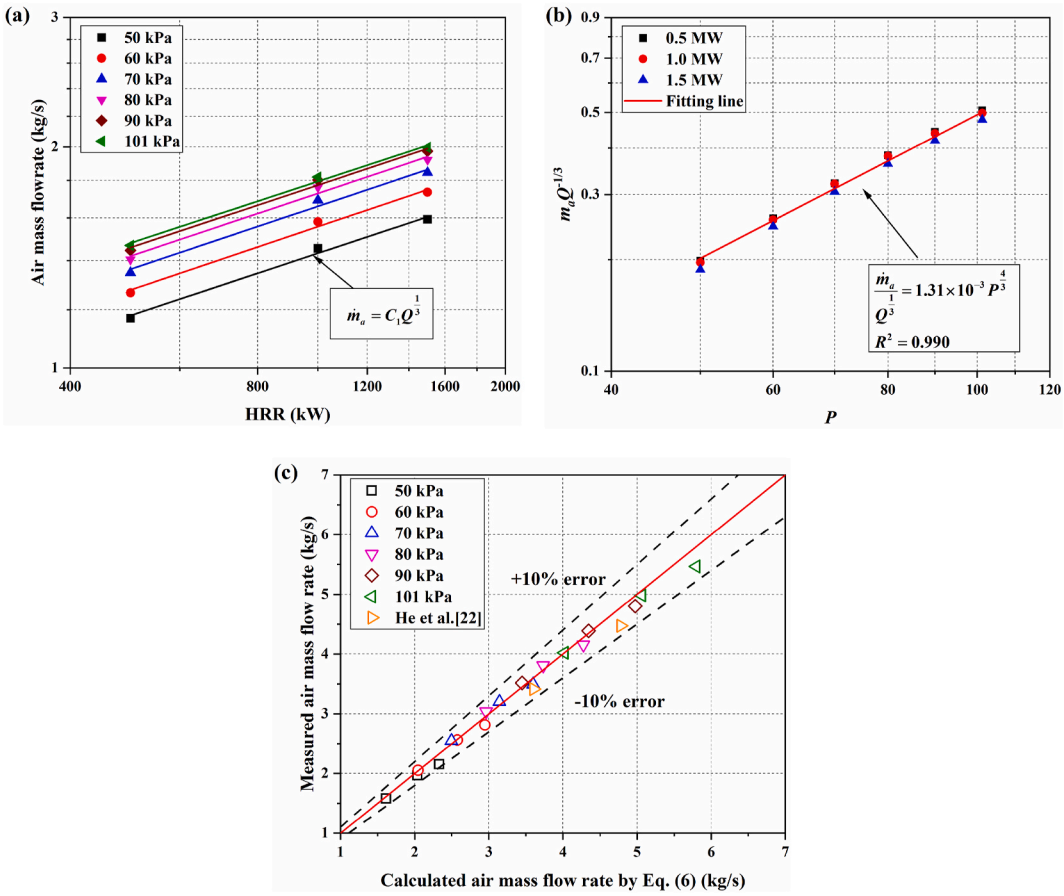

Fig. 6. (a) Correlation between air mass flow rate $\dot{m}_a$ and HRR Q, (b) relationship between $\dot{m}_a/Q^{\frac{1}{3}}$ and ambient pressure P, and (c) comparison between simulated and predicted air mass flow rate using Eq. (6).

Fig. 3(b) plots the flame shapes on the fire floor under different ambient pressures for HRR of 1.5 MW. It can be found that for the same HRR, the flame length increases as the ambient pressure drops, indicating that building fires at lower pressures pose a greater hazard to surrounding combustibles. There are two reasons contributing to the above phenomenon. One is the smaller air density at a lower pressure. In order to entrain more fresh air to sustain the combustion of fire, the flame is stretched to increase the contact area with fresh air, leading to the expansion of the high-temperature zone. The other is the influence of the supplement airflow through the side lobby door. The flame not only tilts toward the stairwell on the vertical plane, but also skews to the left wall on the horizontal plane, as shown in Fig. 4, due to the supplement airflow through the side door. With the decline of the ambient pressure, the air velocity at the lobby door drops, which causes the decrement of the horizontal deflection angle, resulting in that the flame shape size captured by the temperature profile becomes bigger. Therefore, the flame length observed from the temperature is longer at a lower pressure. Besides, as shown in Fig. 3(b), the vertical deflection angle of the flame also declines with the dropping of the pressure, although the decrement in the angle is much small.

The strong supplement air not only facilitates the fire propagation, but also intensifies the burning intensity of the pool fire, which exacerbates the fire hazard. In addition, the mass flow rate of fresh air entering the lobby can represent that of smoke flowing along the stairwell, on account of that the mass flow of fresh air is much greater than the consumption of fuel during the entire fire [22,32]. Fig. 5 (a) plots the variation of air mass flow rates through the lobby door for HRR of 1.5 MW. As shown in Fig. 5(a), the air mass flow rates become stable after a period of time (400 s), showing an average mass flow rate, where a similar phenomenon was also found in previous full-scale fire tests [22].

Fig. 5(b) and (c) present the average mass flow rates and velocities of air through the lobby door during the steady stage for all cases. The air velocity through the lobby door can be calculated as follows

$$V_a = \frac{\dot{m}_a}{C_d \rho_a S} \tag{2}$$

where V_a and $\dot{m}_a$ are the velocity and mass flow rate of fresh air through the lobby door; C_d is discharge coefficient, 0.6–0.8 [33], ρ_a is the density of ambient air at 30 °C, and S is the door area. Fig. 5(b) illustrates that the mass flow rates of air grow approximately

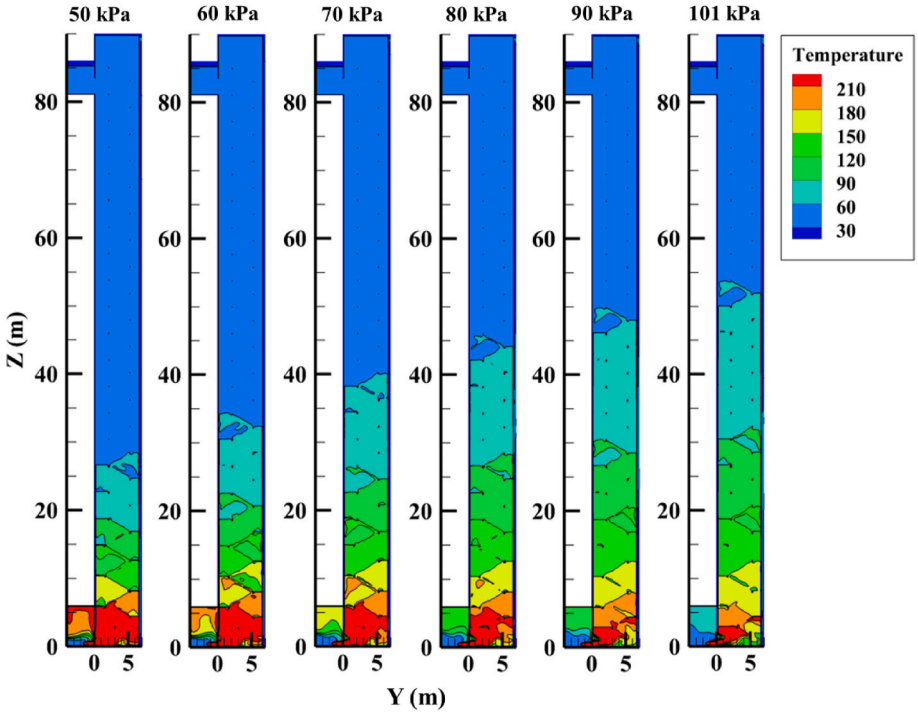

Fig. 7. Temperature profiles at x = 1.35 m in the stairwell under different ambient pressures for HRR of 1.5 MW.

linearly as the ambient pressure rises owning to the increasing density and velocity of fresh air. As Fig. 5(c) shows, the air velocities also increase with the increasing pressure on account of the stronger stack effect at a higher pressure, although the increments in the velocities become smaller with the increasing pressure. As expected, both the velocities and mass flow rates of air increase with the increasing HRR as that (1) fire produce more smoke and (2) a hotter smoke plume enhances the stack effect.

On the basis of the modelling analysis, the air mass flow rate is able to be expressed by the function of ambient pressure P and HRR of the fire source Q as follows

$$\dot{m}_a = f(P, Q) \tag{3}$$

Fig. 6(a) shows the power correlation between the supplement air mass flow rate and HRR with an exponent of $1/3$, and the fitted correlation gives

$$\dot{m}_a = C_1 Q^{\frac{1}{3}} \tag{4}$$

where C_1 is the fitting constant. Then, Eq. (3) can be rewritten as follows

$$\frac{\dot{m}_a}{Q^{\frac{1}{3}}} = C_2 P^{\gamma} \tag{5}$$

where C_2 and γ are fitting constants.

The relationship between $\dot{m}_a/Q^{\frac{1}{3}}$ and P is shown in Fig. 6(b), where the simulation results are in good agreement with Eq. (5) with a correlation coefficient greater than 0.99. The fitted correlation gives

$$\frac{\dot{m}_a}{Q^{1/3}} = 1.31 \times 10^{-3} P^{\frac{4}{3}} \tag{6a}$$

$$\dot{m}_a = 1.31 \times 10^{-3} Q^{\frac{1}{3}} P^{\frac{4}{3}} \tag{6b}$$

A comparison of the measured air mass flow rate from current simulation and previous full-scale experiments [22] and the calculated values using Eq. (6) was conducted in Fig. 6(c). The result illustrates that air mass flow rate is well predicted by Eq. (6), and the maximum error is less than 10%.

3.2. Vertical distribution of smoke temperature, velocity and pressure

Fig. 7 illustrates the temperature profiles at x = 1.35 m in the stairwell under different ambient pressures for HRR of 1.5 MW. It can be observed that as the ambient pressure grows, the temperature near the fire source decreases, while the high-temperature zone in the

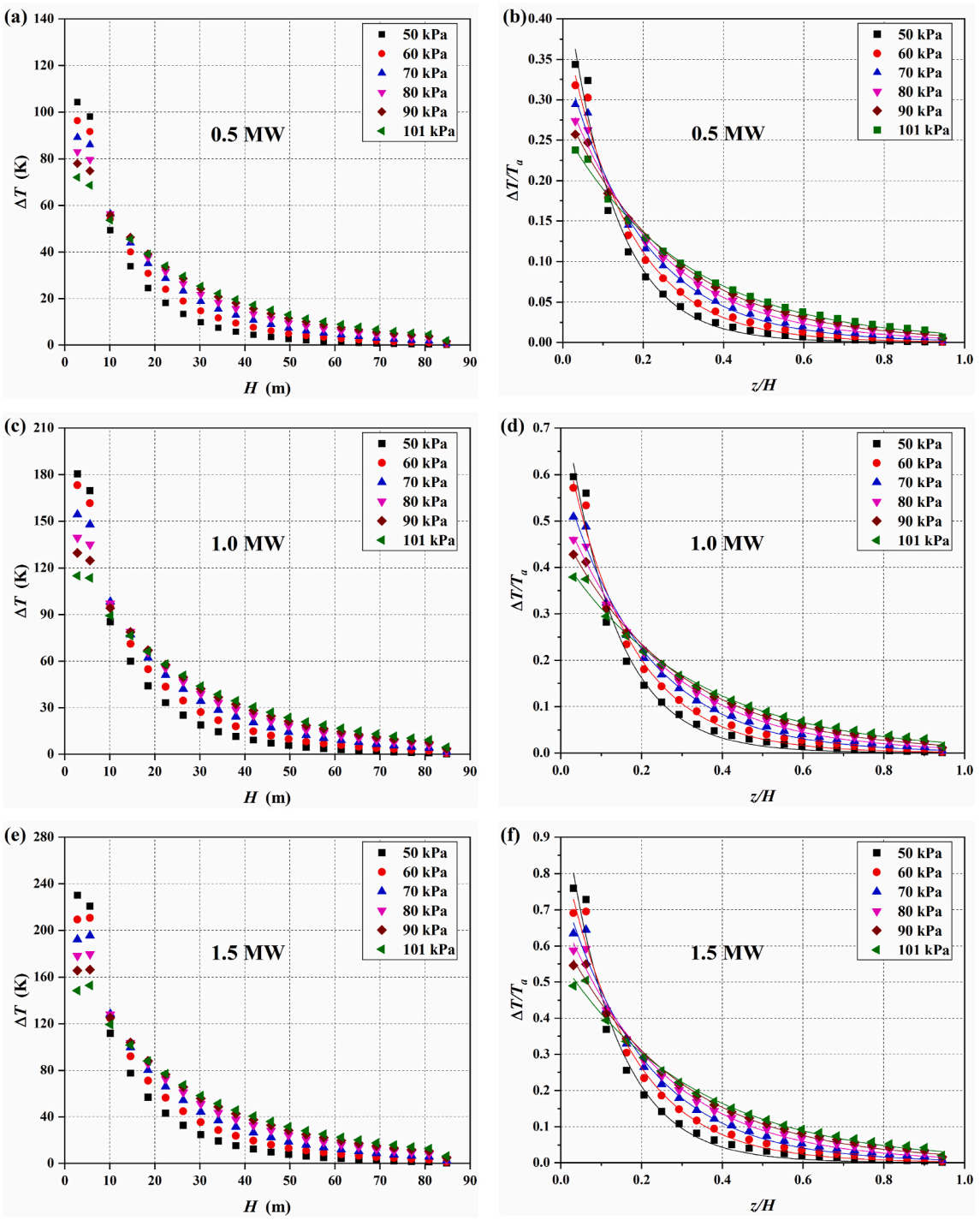

Fig. 8. Vertical temperature distributions for (a, c, e) and normalized temperature rises ($\Delta T/T$) vs. normalized height (z/H) for (b, d, f) at the centerline of the stairwell during the steady-state stage.

stairwell expands continuously. For further investigating the effect of pressure and HRR on temperature distribution of rising smoke, temperatures from the thermocouples during the steady-state stage are used as shown in Fig. 8, where the temperature decreases with the height of the stairwell. For the same HRR of the fire source, there are intersections between the curves of different ambient pressures. The smoke temperature is higher at a lower pressure before the intersection (near the fire source), while it becomes lower after the intersection (away from the fire source). This phenomenon is able to be explained by heat exchanges between hot smoke, inner walls and fire source.

Table 2
Fitted values of α and β and for all cases.

HRR (MW)	Parameters	Ambient pressure (kPa)					
		50	60	70	80	90	101
0.5	α	0.467	0.403	0.356	0.319	0.293	0.265
	β	8.282	6.419	5.186	4.362	3.781	3.336
	R^2	0.985	0.990	0.992	0.995	0.996	0.997
1.0	α	0.802	0.713	0.606	0.531	0.481	0.426
	β	8.011	6.333	4.953	4.109	3.579	3.104
	R^2	0.984	0.989	0.992	0.994	0.995	0.996
1.5	α	1.026	0.881	0.773	0.691	0.627	0.561
	β	7.902	6.051	4.878	4.071	3.515	3.069
	R^2	0.983	0.985	0.988	0.991	0.993	0.994

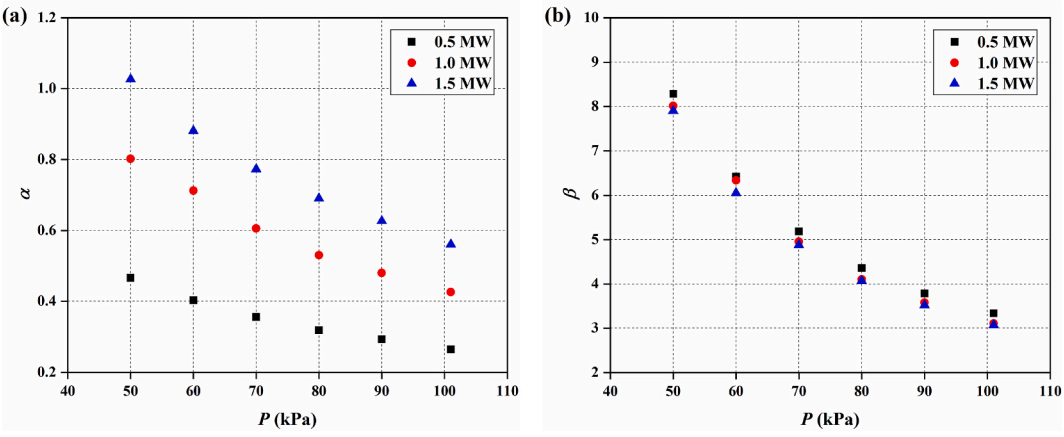

Fig. 9. The fitted values of α and β aganist ambient pressure P.

On the fire floor, the hot smoke is heated by the fire source and the heat released from the flame is mainly transformed into the internal energy of smoke, which results in the temperature rise. The heat exchange can be expressed as follows

$$m_s C_p \Delta T_{ri} = \dot{Q}_c - \dot{Q}_{wall} \tag{7a}$$

where m_s is the smoke mass flow rate in the stairwell, C_p is the specific heat, ΔT_{ri} is the temperatrure rise of the hot smoke, $\dot{Q}_c$ is the convective heat transfer between the fire source and hot smoke, and $\dot{Q}_{wall}$ is heat loss between the hot smoke and inner walls on the fire floor. Because the heat loss is too small to be negligible compared to a huge amount of heat acquired from the fire source. Eq. (7a) can be rewritten as follows

$$\Delta T_{ri} = \frac{\dot{Q}_c}{m_s C_p} \tag{7b}$$

Therefore, for a certain HRR, the smoke temperature rise ΔT_{ri} on the fire floor is directly in connection with the smoke mass flow rate m_s flowing in the stairwell. The smaller the smoke mass flow rate, the higher the smoke temperature rise on the fire floor. From Section 3.1, it can be found that the smoke mass flow rate decreases with the reduced pressure. As a result, the smoke temperature on the fire floor increases with the reduced pressure.

As the height of the smoke rises, the hot smoke is cooled by the cold inner walls, and the internal energy of smoke is transferred to the inner walls, which results in the temperature reduction. The heat exchange can be expressed as follows

$$m_s C_p \Delta T_{re} = \dot{Q}_{wall} = h S_c (T_s - T_{wall}) \tag{8a}$$

$$\Delta T_{re} = \frac{h S_c (T_s - T_{wall})}{m_s C_p} \tag{8b}$$

where h is convective heat transfer coefficient between hot smoke and the inner walls, S_c is convection heat transfer area between hot smoke and the inner walls, and ΔT_{re} is the temperature reduction of the hot smoke.

Consequently, for a certain HRR, the smoke temperature reduction ΔT_{re} is related to the smoke temperature T_s and mass flow rate m_s in the stairwell. On the floors near the fire source, T_s is higher, and m_s is smaller at lower pressure, leading to greater temperature reduction and rapid temperature decay. As the height rise, the smoke temperature difference between lower pressure and higher

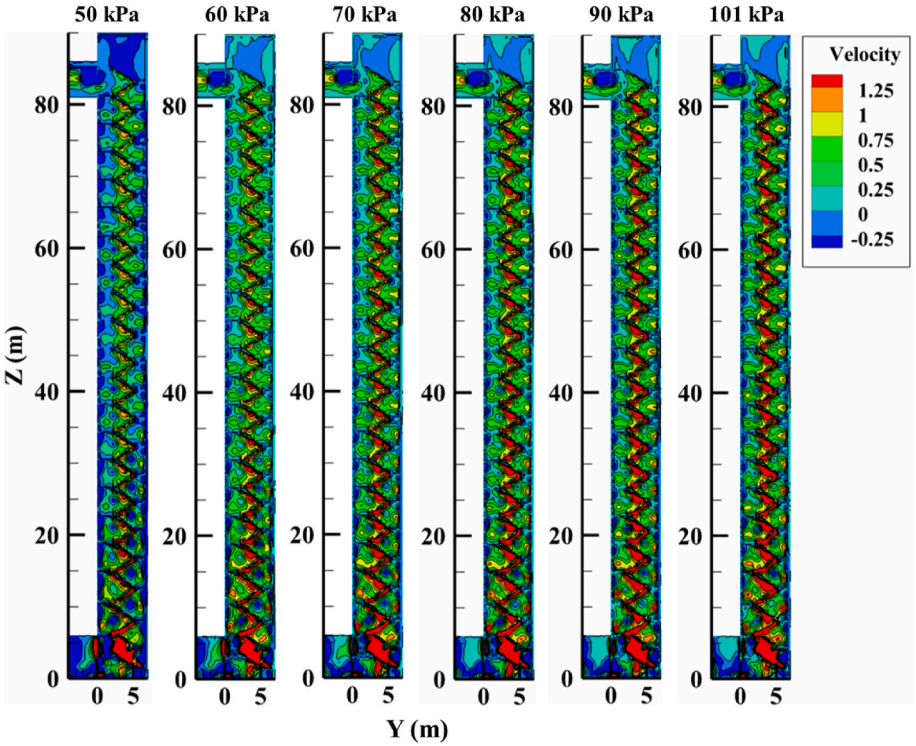

Fig. 10. Velocity profiles at x = 1.35 m in the stairwell under different ambient pressures for HRR of 1.5 MW.

pressure is decreasing; and finally, the smoke temperature at higher pressure would exceed that at a lower pressure which leads to the intersection in temperature curves. In addition, a larger HRR produces a higher temperature under the same ambient pressure.

Fig. 8(b), (d) and (f) show the correlation between normalized temperature ($\Delta T/T_a$) and normalized height (z/H) for all cases, and the temperature data is fitted by Eq. (9), which can be expressed as follows

$$\frac{\Delta T}{T_a} = \frac{T_s - T_a}{T_a} = \alpha e^{-\beta \frac{z}{H}} \tag{9}$$

where T_a and T_s are the temperature of ambient air and hot smoke, α and β are the coefficients which represent the smoke temperature on the fire floor and temperature attenuation in the stairwell, and H is the stairwell height. Table 2 summarizes the fitted values of α and β, where values of determination coefficients R^2 are greater than 0.98, implying the good fitting of temperature data.

Fig. 9(a) and (b) show the values of α and β against the ambient pressure P. As shown in Fig. 9(a), the values of α not only increase with the HRR, but also grow with the ambient pressure, indicating that the HRR and ambient pressure both make great impacts on the smoke temperature on the fire floor. Fig. 9(b) shows that the attenuation coefficient β increases as the ambient pressure declines under the same HRR. It implies a larger temperature attenuation at a lower ambient pressure, which is consistent with the above analyses, while β remains almost constant with HRR at the same pressure, indicating that it is insignificantly influenced by the HRR of fire source.

Fig. 10 plots the velocity profiles at x = 1.35 m in the stairwell under different ambient pressures for HRR of 1.5 MW. It should be noted that the rising velocity here is the vertical component of smoke velocity. As Fig. 10 shows, hot smoke flows spirally in the stairwell, and the high-velocity zone is mainly distributed under the stairs. Although the rising velocity under the landing is relatively small, sometimes negative compared to that under the stairs because of the smoke vortex between the landing and sidewall. In addition, the lower pressure slows down the smoke rising velocity in the stairwell.

Fig. 11 plots the vertical velocity distributions at the centerline of the stairwell during the steady stage for all cases. It can be seen that the smoke rising velocity reaches the maximum at the height of 2.8 m because of the strong plume produced by high temperature flame. Then the smoke plume rises spirally in the stairwell under the block of the stairs and landings, and a sudden decrease in the velocities occurs on the upper region of the ground floor. The velocity increases with the height after the sudden decrease, and reaches another top at the 4th and 5th floors because of the stack effect induced by high-temperature thermal plume which is also observed in the previous studies [3,26]. After the 5th floor, the rising velocity keeps relative stable, indicating a balance between the stack effect induced by thermal plume and block effect by the stairs. The velocity measured by the highest measurement point (84.8 m) is negative, as the upper opening is below the measurement point. In addition, a larger HRR produces a higher velocity because of the stronger stack effect.

Fig. 12 plots the pressure profiles at x = 1.35 m in the stairwell under different ambient pressures for HRR of 1.5 MW. As Fig. 12

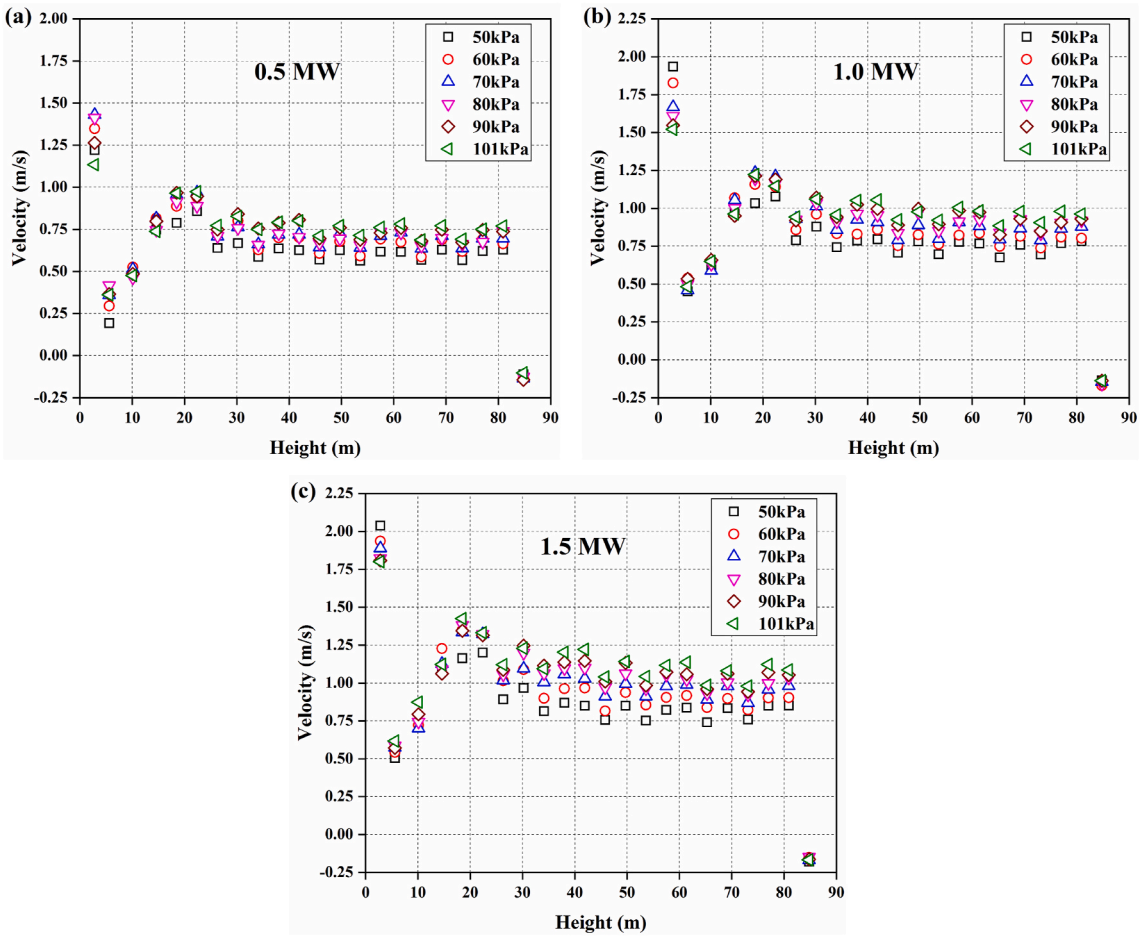

Fig. 11. Vertical velocity distributions at the centerline of the stairwell during the steady-state stage.

shows, the high-pressure zone is mainly distributed in the middle area of the stairwell, and the zone expands as the pressure increases. A negative pressure zone is created near the fire source because of the expansion of high temperature smoke produced by fire, which results in a lower density of smoke compared to that of cold air outdoor. And the area of the negative pressure zone also increases with the increasing ambient pressure. A neutral pressure plane occurs where the pressure difference between the cold air outside and hot smoke inside of the stairwell is zero, and its maximum height can be obtained from the above pressure profiles. Table 3 lists the maximum heights of neutral pressure plane for all cases. It can be seen that the neutral pressure plane is mainly located near the fire source (1 F and 2 F). The height of the neutral pressure plane both increases with HRR and ambient pressure, but it is more susceptible to the ambient pressure than the HRR of the fire source.

Fig. 13 shows vertical pressure distributions at the centerline of the stairwell during the steady-state stage for all cases. It can be found that the pressure initial increases with the height, but decreases after it reaches the maximum at the middle area of the stairwell because of the pressure relief of the upper opening. The values of negative pressures on the fire floor increase with the increasing HRR and ambient pressure, resulting in the stronger stack effect for larger HRRs at higher pressures. The height of the maximum pressure increases with the ambient pressure, and the value also increases as the ambient pressure grows. While for different HRRs, the height of maximum pressure is constant, but the value increases with HRR because of the higher temperature in the stairwell.

3.3. Smoke rising time

Fig. 14 (a), (b) and (c) plot the increasing height of the smoke disturbance front versus the rising time with varying HRRs and ambient pressures. It can be seen that the rising time used for the smoke disturbance front to get to the upper opening decreases as the HRR increases under the same ambient pressure, and for the same HRR, it increases as the ambient pressure drops.

The rising time for smoke disturbance front to get to increasing height is expressed as follows

$$t = \int_0^z \frac{1}{V_z} dz = \int_0^z \frac{\rho_z A}{\dot{m}_s} dz \tag{10}$$

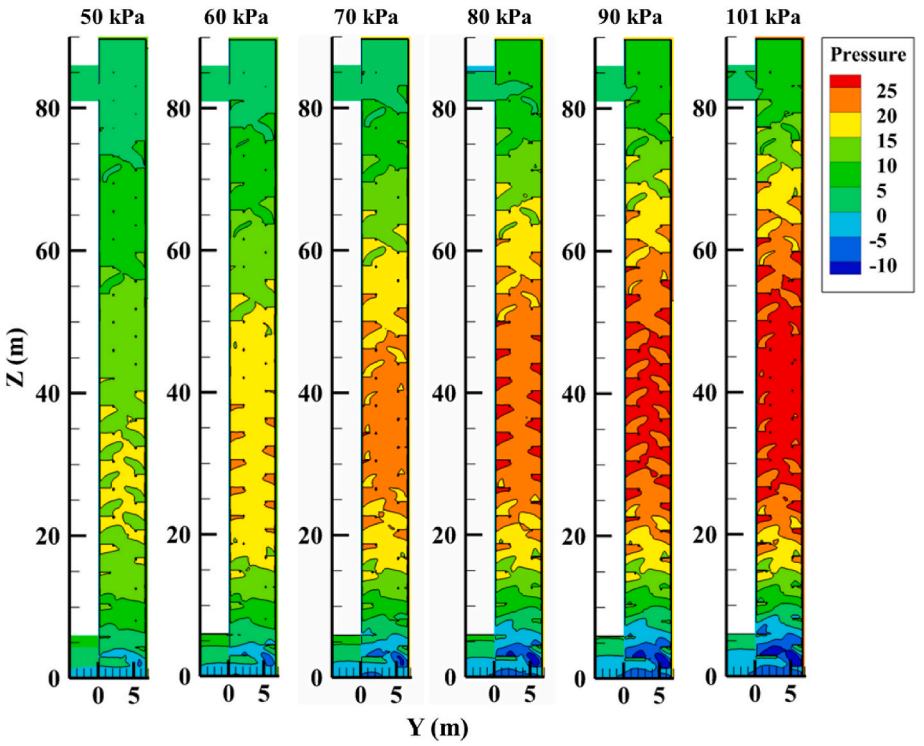

Fig. 12. Pressure profiles at x = 1.35 m in the stairwell under different ambient pressures for HRR of 1.5 MW.

Table 3
The maximum heights of neutral pressure plane in the stairwell.

HRR (MW)	Ambient pressure (kPa)					
	50	60	70	80	90	101
0.5	3.54 m	4.05 m	4.56 m	4.84 m	6.01 m	7.58 m
1.0	4.17 m	4.79 m	5.87 m	7.51 m	7.95 m	8.43 m
1.5	4.17 m	5.20 m	6.11 m	8.01 m	8.47 m	8.63 m

where V_z and ρ_z is the velocity and density of smoke at height z, repsectively. From the ideal gas law, we have

$$\rho_z = \frac{P}{RT_z} \tag{11}$$

Combining Eqs. (9)–(11), it yields

$$t = \frac{PA}{RT_a\dot{m}_s}\int_0^z \frac{1}{1+\alpha e^{-\beta\frac{z}{H}}}dz = \frac{PHA}{RT_a\beta\dot{m}_s} ln\frac{1+\alpha e^{-\beta\frac{z}{H}}}{(1+\alpha)e^{-\beta\frac{z}{H}}} \tag{12}$$

Based on Section 3.1, the smoke mass flow rate in the stairwell is approximately equivalent to that of air through the lobby door. Therefore, the correlation between the rising time and arrival height of hot smoke can be expressed as

$$t = \frac{PHA}{RT_a\beta\dot{m}_a} ln\frac{1+\alpha e^{-\beta\frac{z}{H}}}{(1+\alpha)e^{-\beta\frac{z}{H}}} \tag{13}$$

So as to verify the accuracy of the above equation, it is not only compared to the simulated results by CFD code, but also the results from both small-scale and full-scale experiments under normal pressure. Table 4 lists the detailed conditions of previous experiments, consisting of the fire source, HRR, ambient pressure, and stairwell size. Fig. 14(d) shows the comparisons of the measured rising time and predicted rising time by Eq. (13). It can be observed that the rising time predicted by Eq. (13) agrees well with the simulated results by FDS and experiment results from previous studies.

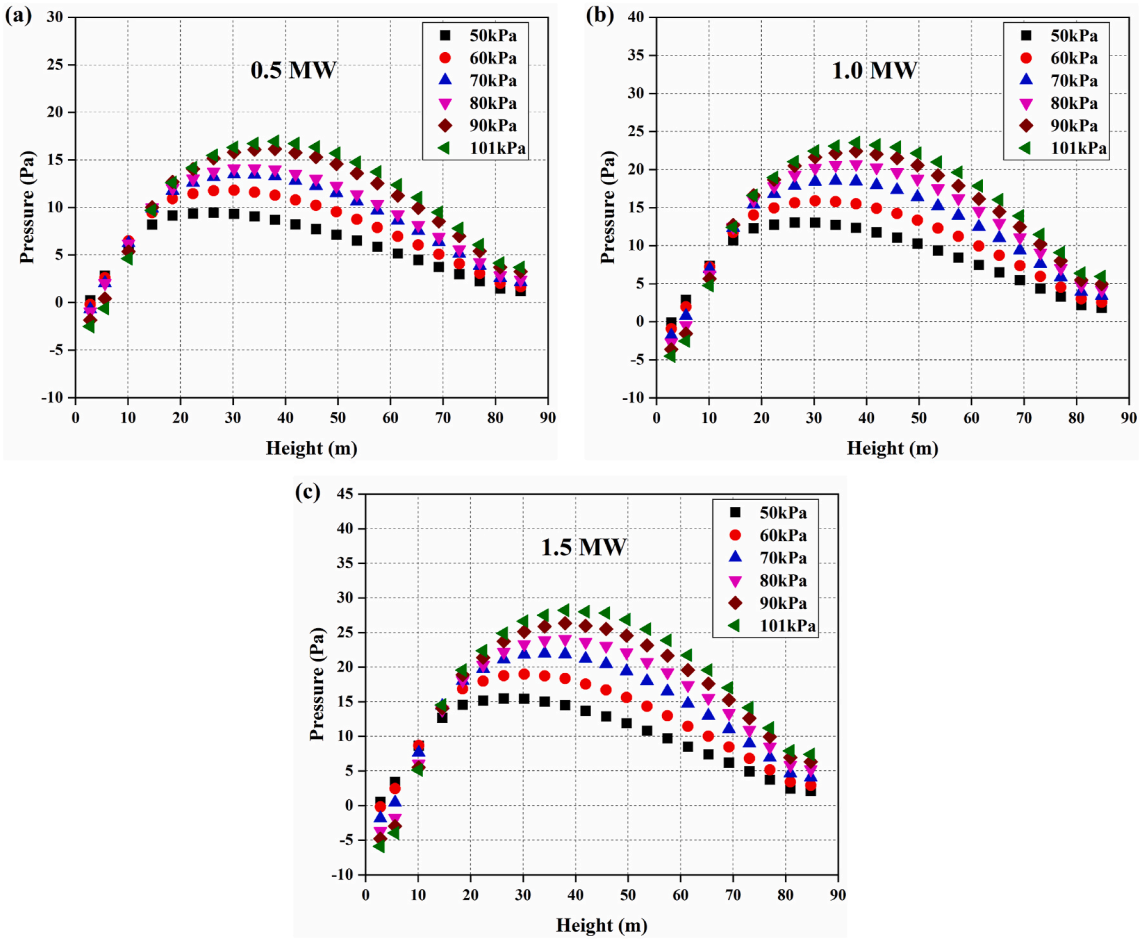

Fig. 13. Vertical pressure distributions at the centerline of the stairwell during the steady-state stage.

4. Conclusion

This work conducts a sequence of full-scale simulations with varying HRRs of fire source and ambient pressures to investigate smoke dynamics in stairwell fires. During fires, the high-temperature region gradually moves from the lobby to the stairwell, driven by the stack effect. The flame length increases with the decrease of ambient pressures, indicating that the fire at a lower pressure poses a greater hazard. The air mass flow rate decreases as the ambient pressure drops because of the decreasing density and velocity of fresh air as a result of the weakened stack effect. While it increases with the increasing HRR as that (1) fire produces more smoke, and (2) a hotter smoke plume enhances the stack effect. Furthermore, the relationship between air mass flow rate, HRR, and ambient pressure is put forward.

The temperature of hot smoke near the fire source in general increases as the ambient pressure drops. However, on the floors away from the fire source, the temperature decreases with the reduced pressure, due to the higher temperature attenuation at lower pressures. The velocity and hot pressure of smoke in the stairwell both decline as the ambient pressure drops on account of the weakened stack effect. The height of the neutral pressure plane is more susceptible to the ambient pressure than the HRR of the fire source. Based on theoretical analysis, a uniform correlation of the rising time and arrival height of the smoke plume front is found, and the correlation agrees with simulated results with varying ambient pressures and previous test results at the normal pressure.

CRediT author statement

Junjang He: Investigation, Writing - Original Draft, Formal analysis **Xinyan Huang:** Conceptualization, Writing - Review & Editing **Xiaoyao Ning:** Investigation, Resources **Tiannian Zhou:** Investigation, Resources **Jian Wang:** Supervision **Rechard Kwok Kit Yuan:** Review & Editing.

Declaration of competing interest

The authors declare that they have no known competing financial interests or personal relationships that could have appeared to

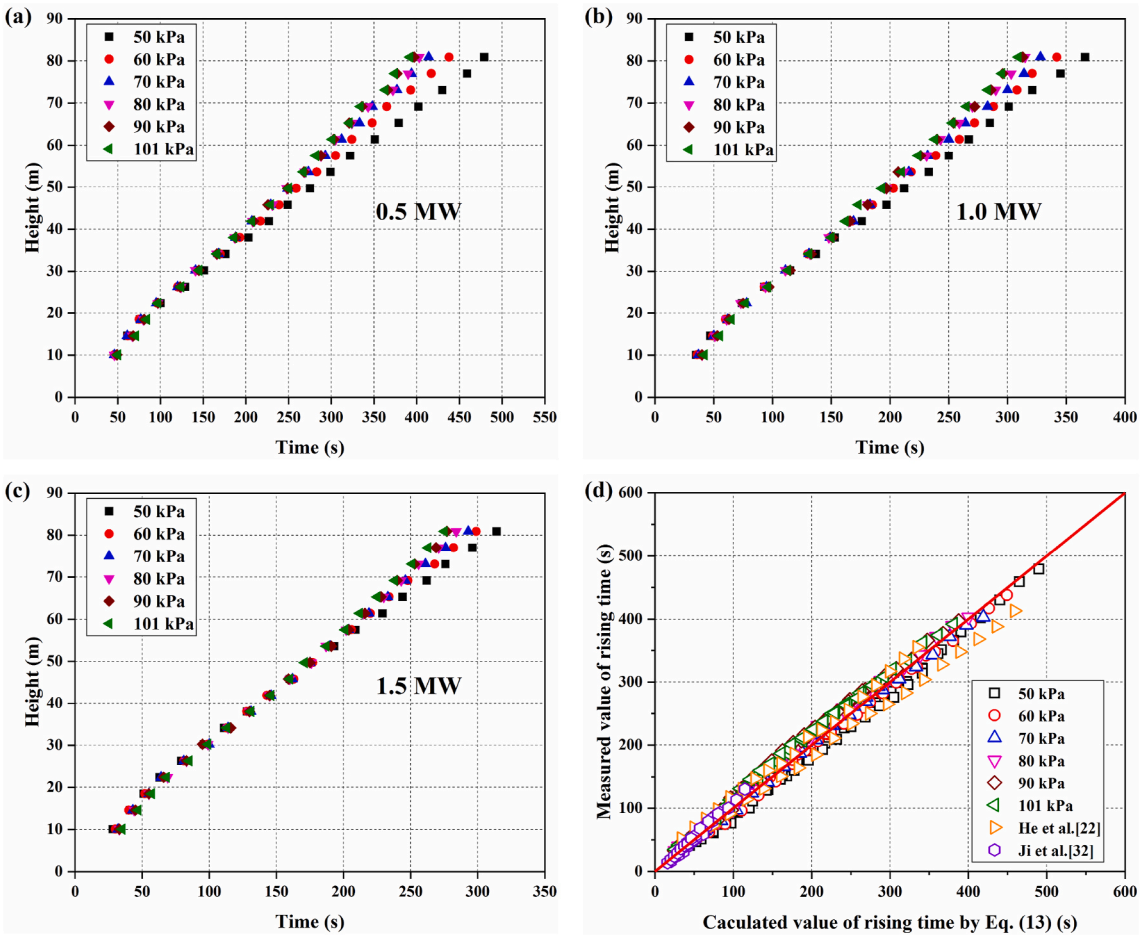

Fig. 14. Increasing heights of the smoke aganist time, (a) 0.5 MW fire, (b) 1.0 MW fire, (c) 1.5 MW fire and (d) comparison of measured rising time and predicted rising time by Eq. (13).

Table 4
Detailed conditions of the previous experiments.

Experiment scale	Fire source	HRR (MW)	Ambient pressure (kPa)	Stairwell size
Full scale [22]	Ethanol	0.36, 0.84	101	6.5 m (length) × 2.7 m (width) × 89.7 m (height)
Small scale [32]	Methanol	/	101	1.5 m (length) × 1.0 m (width) × 12.6 m (height)

influence the work reported in this paper.

Acknowledgments

This work is supported by National Key R&D Program of China (No. 2018YFC0809500), Fundamental Research Funds for the Central Universities (No. WK2320000052), and Key R&D Program of Yunnan Province (No. 202003AC100001).

References

[1] W.K. Chow, Design Fire in Performance-Based Fire Safety Design for Green and Sustainable Buildings, PLEA 2006 - 23rd International Conference on Passive and Low Energy Architecture, Conference Proceedings, 2006, pp. II431–II436.
[2] Y. Chen, X. Zhou, T. Zhang, Y. Hu, L. Yang, Turbulent smoke flow in evacuation staircases during a high-rise residential building fire, Int. J. Numer. Methods Heat Fluid Flow 25 (3) (2015) 534–549.
[3] C.S. Ahn, D.Y. Kim, C. Park, M.W. Kim, T. Kim, B.H. Bang, S. An, A.L. Yarin, S.S. Yoon, Experimental and numerical study of smoke behavior in high-rise stairwells with open and closed windows, Int. J. Therm. Sci. 157 (2020).
[4] Y. Alarie, Toxicity of fire smoke, Crit. Rev. Toxicol. 32 (4) (2002) 259–289.
[5] A.A. Stec, T.R. Hull, Assessment of the fire toxicity of building insulation materials, Energy Build. 43 (2–3) (2011) 498–506.
[6] R. Priyadarsini, K. Cheong, N. Wong, Enhancement of natural ventilation in high-rise residential buildings using stack system, Energy Build. 36 (1) (2004) 61–71.

[7] J. Zhang, W. Lu, R. Huo, R. Feng, A new model for determining neutral-plane position in shaft space of a building under fire situation, Build. Environ. 43 (6) (2008) 1101–1108.
[8] D. Yang, T. Du, S. Peng, B. Li, A model for analysis of convection induced by stack effect in a shaft with warm airflow expelled from adjacent space, Energy Build. 62 (2013) 107–115.
[9] J. Lee, D. Song, D. Park, A study on the development and application of the E/V shaft cooling system to reduce stack effect in high-rise buildings, Build. Environ. 45 (2) (2010) 311–319.
[10] C.H. Su, Y.C. Lin, C.M. Shu, M.C. Hsu, Stack effect of smoke for an old-style apartment in Taiwan, Build. Environ. 46 (12) (2011) 2425–2433.
[11] Y. Chen, X. Zhou, T. Zhang, Z. Fu, Y. Hu, L. Yang, Numerical analysis of combined buoyancy-induced and pressure-driven smoke flow in complex vertical shafts during building fires, Int. J. Numer. Methods Heat Fluid Flow 26 (6) (2016) 1684–1698.
[12] D. Li, T. Zhou, Z. Liu, J. Wang, Transport phenomena of fire-induced smoke flow in a semi-open vertical shaft, Int. J. Numer. Methods Heat Fluid Flow 28 (11) (2018) 2664–2680.
[13] W.Z. Black, Smoke movement in elevator shafts during a high-rise structural fire, Fire Saf. J. 44 (2) (2009) 168–182.
[14] W.X. Shi, J. Ji, J.H. Sun, S.M. Lo, L.J. Li, X.Y. Yuan, Influence of fire power and window position on smoke movement mechanisms and temperature distribution in an emergency staircase, Energy Build. 79 (2014) 132–142.
[15] G.I. Taylor, The instability of liquid surfaces when accelerated in a direction perpendicular to their planes. I, Proc. Roy. Soc. Lond. Math. Phys. Sci. 201 (1065) (1950) 192–196.
[16] M.J. Andrews, D.B. Spalding, A simple experiment to investigate two-dimensional mixing by Rayleigh–Taylor instability, Phys. Fluid. Fluid Dynam. 2 (6) (1990) 922–927.
[17] N.R. Marshall, The behaviour of hot gases flowing within a staircase, Fire Saf. J. 9 (3) (1985) 245–255.
[18] N.R. Marshall, Air entrainment into smoke and hot gases in open shafts, Fire Saf. J. 10 (1) (1986) 37–46.
[19] W.X. Shi, J. Ji, J.H. Sun, S.M. Lo, L.J. Li, X.Y. Yuan, Influence of staircase ventilation state on the airflow and heat transfer of the heated room on the middle floor of high rise building, Appl. Energy 119 (2014) 173–180.
[20] Z. Gao, X. Yuan, J. Ji, Y. Li, L. Yang, Influence of stack effect on flame shapes of gas burner fires, Appl. Therm. Eng. 127 (2017) 1574–1581.
[21] L. Zhu, X. Yuan, Z. Gao, J. Ji, Experimental investigation of effect of external side wind on fire behaviors in a corridor connected to a shaft, Fire Technol. 56 (2) (2020) 863–881.
[22] J. He, X. Huang, X. Ning, T. Zhou, J. Wang, R. Yuen, Stairwell smoke transport in a full-scale high-rise building: influence of opening location, Fire Saf. J. 117 (2020).
[23] M. Li, Z. Gao, J. Ji, K. Li, Modeling of positive pressure ventilation to prevent smoke spreading in sprinklered high-rise buildings, Fire Saf. J. 95 (2018) 87–100.
[24] K. McGrattan, S. Hostikka, R. McDermott, J. Floyd, C. Weinschenk, K. Overholt, Fire dynamics simulator user's guide, NIST - Spec. Publ. 1019 (6) (2013).
[25] G. Hadjisophocleous, Q. Jia, Comparison of FDS prediction of smoke movement in a 10-Storey building with experimental data, Fire Technol. 45 (2) (2009) 163–177.
[26] X.Q. Sun, L.H. Hu, Y.Z. Li, R. Huo, W.K. Chow, N.K. Fong, G.C.H. Lui, K.Y. Li, Studies on smoke movement in stairwell induced by an adjacent compartment fire, Appl. Therm. Eng. 29 (13) (2009) 2757–2765.
[27] G. Zhao, T. Beji, B. Merci, Study of FDS simulations of buoyant fire-induced smoke movement in a high-rise building stairwell, Fire Saf. J. 91 (2017) 276–283.
[28] C.S. Ahn, B.H. Bang, M.W. Kim, S.C. James, A.L. Yarin, S.S. Yoon, Theoretical, numerical, and experimental investigation of smoke dynamics in high-rise buildings, Int. J. Heat Mass Tran. 135 (2019) 604–613.
[29] L. Li, Y. Li, Z. Wu, P. Xu, X. Peng, H. Wang, C. Fan, Window ejected thermal plume dispersion and recirculation behavior in urban street canyon with different building height ratios under wind, Case Stud. Therm. Eng. 27 (2021).
[30] Y. He, C. Jamieson, A. Jeary, J. Wang, Effect of Computation Domain on Simulation of Small Compartment Fires, Fire Safety Science, 2008, pp. 1365–1376.
[31] C. Rew, D. Deaves, Fire spread and flame length in ventilated tunnels-a model used in Channel tunnel assessments, in: Proceedings of the International Conference on Tunnel Fires and Escape from Tunnels, Independent Technical Conferences Ltd., Lyon, France, 1999, pp. 397–406.
[32] J. Ji, L.J. Li, W.X. Shi, C.G. Fan, J.H. Sun, Experimental investigation on the rising characteristics of the fire-induced buoyant plume in stairwells, Int. J. Heat Mass Tran. 64 (2013) 193–201.
[33] J.A. Rockett, Fire induced gas flow in an enclosure, Combust. Sci. Technol. 12 (4–6) (1976) 165–175.